Self-diffusion in high-purity α-Al_2O_3: Comparison of Ti-doped, Mg-doped and undoped single crystals

Peter Fielitz[1*], Steffen Ganschow[2], Klemens Kelm[3], Günter Borchardt[1]

[1] Technische Universität Clausthal, Institut für Metallurgie, Robert-Koch-Str. 42, D-38678 Clausthal-Zellerfeld, Germany

[2] Leibniz-Institut für Kristallzüchtung, Max-Born-Str. 2, D-12489 Berlin, Germany

[3] Deutsches Zentrum für Luft- und Raumfahrt, Institut für Werkstoff-Forschung, Linder Höhe, D-51147 Köln, Germany

* corresponding author: e-mail: peter.fielitz@tu-clausthal.de

Dedicated to Professor Stanislas Scherrer on the occasion of his 88th birthday.

Abstract

Oxygen diffusivity in α-alumina is characterised by a scatter band of about one decade and a half in an Arrhenius diagram. In order to control decisive material parameters the present study is based on high-purity single crystals which were deliberately doped with aliovalent elements (Mg or Ti) and simultaneously annealed in an $^{18}O_2$ atmosphere (200 mbar at 1650 °C). In such a crucial experiment the diffusivities in undoped and acceptor or donor doped alumina are identical within a factor of about 2. Contradictory findings in the past on the impact of Mg and Ti on the oxygen diffusion can be rationalised due to published similar calculated energies for the most probable dopant incorporation reactions. Al self-diffusion is much more rapid than oxygen diffusion in undoped and Ti-doped α-alumina. In this work we show for the first time that Mg doping drastically reduces the Al diffusivity in α-alumina.

Key words: alumina; Ti-doped; Mg-doped; tracer diffusion; SIMS

1 Introduction

Alumina is an important ceramic material with various technological applications ranging from opto-electronics to harsh environments at high temperatures. As sintering, creep, and growth of protective alumina scales directly correlate with the diffusion of the constituent elements research on the transport of oxygen and aluminium at high temperatures is being promoted since decades [1]-[4].

Beside its technological importance α-alumina is a unique model material: Because of its extremely low concentrations of intrinsic point defects at thermodynamic equilibrium [5] it can be considered as a (nearly) “perfect” crystalline oxide as for as point defects in thermodynamic equilibrium are considered. This feature permits to study the impact of deliberate doping of high-purity alumina without interference from unwanted impurities. It further creates a basis to take into consideration non-equilibrium point defects due to technical boundary conditions of conventional crystal growth processes [6]. In many earlier studies this aspect could obviously not always be considered.

In 2011 Heuer et al. [7] compiled the best available bulk diffusivity data for oxygen and aluminium in Al_2O_3. The scatter of the oxygen diffusion data reflects the presumably pronounced differences between the respective single crystals used in the evaluated experiments as far as type and content of impurities are concerned. Heuer's findings (p. 148 in [7]) can be summarized as follows: None of the crystals used for the published oxygen diffusion studies should show intrinsic behaviour. Their native point defect population was virtually too low for detectable intrinsic diffusion. This view seems to be in agreement with Kröger's [8] interpretation. The scatter band of the oxygen diffusion results in a conventional Arrhenius plot with a span of nearly one decade and a half. According to Heuer et al. [3],[7],[9] this behaviour could be rationalised if one postulates that alumina is principally "buffered" with regard to the oxygen vacancy concentration.

This conjecture motivated the present authors to check its validity. For this purpose high-purity single crystals with an unprecedented low concentration of the usual impurities were grown. For the diffusion experiments undoped and deliberately doped crystals were produced, using only Ti and Mg as “impurities”, whose concentrations were exactly known. In order to assure the required quality of the crystals a direct collaboration with experienced crystal growers (Leibniz Institute for Crystal Growth, Berlin, Germany) was installed whereby it was guaranteed that all the undoped as well as the doped crystals had the same history. Such a procedure yields a perfect comparability of the used crystals and the diffusion data obtained in the experiments.

2 Experimental procedures

One goal of our investigation was to supply reliable data for the diffusion of aluminium in α-alumina with various Ti-doping levels. The respective results and their interpretation can be found elsewhere [6], as well as the applied experimental procedure. Simply in order to facilitate

understanding the present publication the essential features of the experimental work will be summarized in the following.

2.1 Crystal growth and doping

Single crystals were grown using the Czochralski technique with induction heating. The starting material consisting of premelted granules of Al_2O_3 (Spolchemie, ~5N purity) doped with an appropriate amount of MgO was melted in a 40 ml cylindrical iridium crucible. An active afterheater was placed on top of the crucible to create above the melt a thermal cavity into which the crystal was pulled. The crucible/afterheater arrangement was enclosed in alumina and zirconia ceramic elements for additional thermal insulation. For technical details the reader is referred to [6].

Table 1 Planned and analysed dopant concentrations of the single crystals grown for this investigation. Details concerning the growth of Ti-doped single crystals and the chemical element analysis using an Inductively Coupled Plasma (ICP) spectrometer or a Glow Discharge Mass Spectrometer (GDMS) are given elsewhere [6].

Ti-doped	planned [wt ppm]	300	600	900	1200
	ICP [wt ppm]	**263 ± 5**	**593 ± 10**	**1010 ± 20**	**1100 ± 20**
Mg-doped	planned [wt ppm]	125	250	-	-
	GDMS [wt ppm]	**37**	**66**	-	-

Table 2 Concentration (wt ppm) of elements which are above the detection limit of a GDMS analysis in an undoped, Ti-doped and Mg-doped α-Al_2O_3 single crystal.

	B	Na	**Mg**	Si	P	S	Cl	K	Ca	**Ti**	Cr
Undoped	0.09	0.53	0.08	1.4	2.6	2.3	0.53	1.1	1.1	< 0.05	< 0.5
Ti-doped	0.07	0.47	0.63	1.9	3.4	1.3	0.63	1.0	1.1	**580**	< 0.5
Mg-doped	0.10	0.95	**66**	1.9	2.4	1.7	0.69	1.6	1.2	0.11	7.1

Unfortunately, the Mg distribution coefficient in sapphire is unknown. The observable Mg distribution in a grown crystal is caused by an effective distribution coefficient that is strongly

affected by growth conditions, in particular growth velocity and melt mixing, e.g. by convection. From Mg distribution data in this study we can estimate the effective distribution coefficient to be in the range 0.2 - 0.3. All planned and analysed dopant concentrations of this comparative study are shown in Table 1 (including the Ti-doped samples of the earlier publication [6] for comparison).

Because of its sensitivity at the sub-ppm level for almost all elements in the periodic table Glow Discharge Mass Spectrometry (GDMS) was used to control the purity of the crystals as well as the dopant concentrations [10]. A full scan GDMS analysis (Evans Analytical Group SAS, Toulouse, France) includes 75 elements (except C, N, O, H). The detection limit is in the range from 0.01 to 0.5 wt ppm (except Fe < 1, Ge < 1, Nb < 50, Mo < 20, W < 20 wt ppm). Table 2 presents the concentrations of those impurities in an undoped, in a Ti-doped and in a Mg-doped α-Al_2O_3 single crystal which are above the detection limit of the GDMS analysis. Obviously, the concentrations of the detectable impurities (B, Na, Si, P, S, Cl, K, Ca, Cr) are similar in all three samples and practically not influenced by the doping of the single crystals. However, there are three exceptions (Mg, Ti, Cr). In the undoped sample the Mg impurity concentration is 0.08 wt ppm, but it increased by a factor of about ten (0.63 wt ppm) in the Ti-doped sample. On the other hand, doping with MgO caused a slight Ti contamination (0.11 wt ppm) and a significant Cr contamination (7.1 wt ppm) of the sample, which, however, will be incorporated substitutionally without introducing charge compensating point defects.

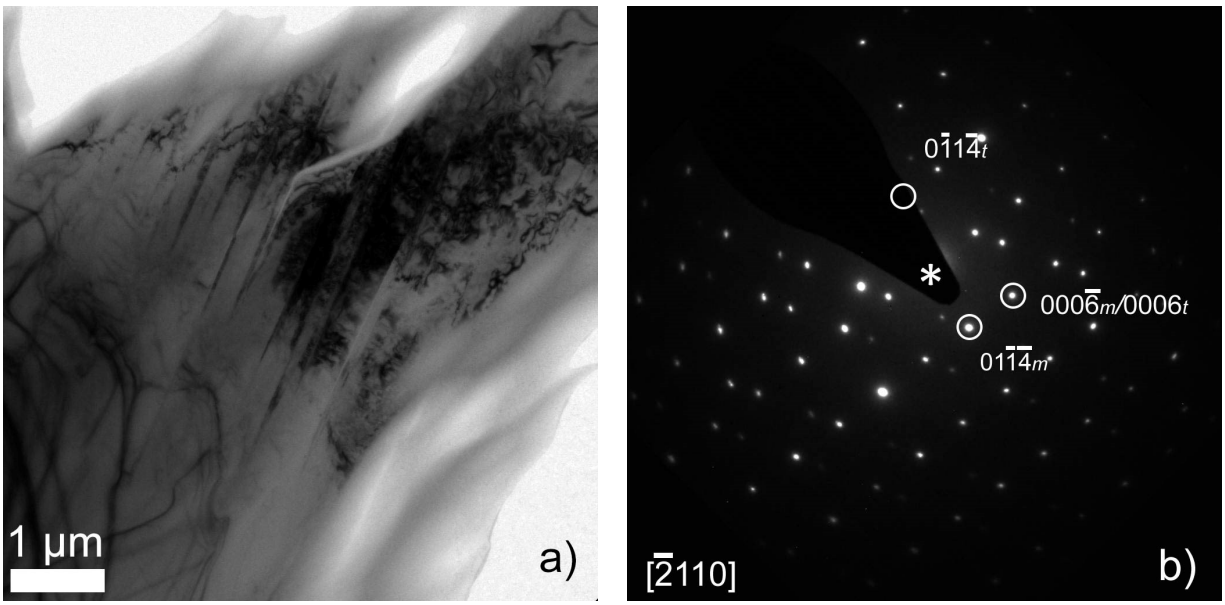

Fig. 1 (a) Sample area of the 66 ppm Mg-doped sample depicting polysynthetic basal twinning. (b) SAED pattern of the area in (a) with beam along the corundum a-axis.

2.2 TEM analysis

The preparation of the samples for the transmission electron microscopy (TEM) investigations was performed according to the state of the art procedures described in more detail in [6]. For the final thinning step the samples were mounted in a standard sample holder made of titanium and were ion-polished at an acceleration voltage of 4 keV (PIPS Model 691, Gatan Inc., USA) until a hole with rims transparent to the electron beam was obtained. The sample was etched from the back side, applying only slight ion beam cleaning from the front side to remove redeposition layers.

A Philips Tecnai F30 transmission electron microscope (Philips Electron Optics, The Netherlands) operating at 300 keV was used for the TEM investigations. The system is equipped with a STEM system as well as an EDAX Apollo XLT windowless detector (EDAX Inc., USA). Images were recorded on a bottom-mounted CCD camera (Gatan CCD 694, Gatan Inc., USA). Imaging of the samples was carried out in TEM mode.

No precipitates (MgO or $MgAl_2O_4$) could be detected in the sample doped with 66 ppm of magnesium. While most of the Mg-doped single crystal appears as defect-free, some distortion bands were observed running along the [0001] direction. While they were observable even in low magnification and in the optical microscope they appeared as stacks of planar defects at medium magnifications (Fig. 1a).

The selected electron diffraction pattern (SAED) revealed basal twinning within these regions (Fig. 1b), which was also confirmed by lattice plane imaging. Thus, the stacked planar structures are polysynthetic twins with (0001) as the twinning as well as the interface plane. For basal twins, different structural models are discussed (see [11], [12]), usually employing lattice relaxations near the interface. Thus, a stack of twins might act as a fast diffusion path.

The level of dopants in the samples used in this study is too low for a proper detection by EDS in the transmission electron microscope. Usually, by careful measurement about 10000 ppm of Mg should be detectable. Such concentrations can be reached especially in precipitates or enrichment zones, making EDS analysis possible. EDS analysis of the polysynthetic twins revealed no enrichment of Mg either, but it remains unclear if such an enrichment would surpass the detection limit.

The samples doped with titanium were exceptionally homogeneous. TEM investigations could not find an indication of dislocation structures (see [6]).

2.3 Diffusion experiments

The samples (about 1 mm thick and 15 mm in diameter), cut perpendicular to the growth axis (a-axis), were polished to optical flatness with diamond paste of decreasing particle size (15, 6, 3, 1 µm). After ultrasonic cleaning in ethanol the samples were pre-annealed in 200 mbar $^{16}O_2$ gas at 1650 °C for 9 hours to remove polishing damage. The nominally undoped as-grown samples were colourless and remained colourless after pre-annealing. The Ti-doped as-grown samples were light pink with increasing colour intensity as the doping increased. After the pre-annealing step all Ti-doped samples became colourless which indicates that Ti^{3+} oxidised to Ti^{4+} during pre-annealing [13]. The Mg-doped as-grown samples were colourless and became orange after pre-annealing [14]. After pre-annealing, a thin layer of $^{26}Al_2O_3$ was deposited on an area of 2×2 mm^2 of the sample surface (see [6] and [15] for details). The layer consists of an approximately homogeneous distribution of small $^{26}Al_2O_3$ particles (size about 100 nm) with a very low specific activity [16]. The diffusion experiments were performed in 200 mbar oxygen gas atmosphere using a special tube furnace (see ref. [17] for a detailed description of the tube furnace and the diffusion annealing procedure).

Depth distributions of the isotopes ^{26}Al and ^{18}O were determined by Secondary Ion Mass Spectrometry (SIMS) using a Cameca IMS 3f instrument. A 14.5 keV O^- primary beam was applied with a current of about 150 nA and a 50 µm spot size. The raster-scanned area was 250×250 µm^2 and the diameter of the analysed zone was 60 µm. Positive secondary ions were used in the analysis of the samples. Sample charging was prevented by coating the sample surface with a 50 nm thick carbon film.

To evaluate the diffusion coefficient from the measured depth profiles the solution of the diffusion equation for a constant diffusion source $\left(c_0 = \text{constant}\right)$ located at $x = 0$ was used [18]

$$c(x) - c_\infty = \left(c_0 - c_\infty\right) \operatorname{erfc}\left(\frac{x}{L}\right) \quad \text{with} \quad L = 2\sqrt{D \cdot t} \tag{1}$$

where L is the diffusion length, D the diffusion coefficient and t the annealing time at the diffusion temperature. The concentration c_∞ at $x = \infty$ corresponds to the background value of the tracer isotope. The applicability of this solution for the granular $^{26}Al_2O_3$ tracer layer was demonstrated elsewhere [15].

3 Results

In order to be able to show directly how Ti and Mg doping affects the mobility of oxygen, 4 samples (undoped, 37 wt ppm Mg, 593 wt ppm Ti, 1100 wt ppm Ti) were annealed simultaneously during the pre-annealing step and the diffusion annealing step. Pre-annealing was performed in 200 mbar $^{16}O_2$ gas at 1650 °C for a duration appreciably longer (48 h) than the diffusion time. After that the ^{18}O exchange experiment was performed for 24 h at 1650 °C in 200 mbar $^{18}O_2$ gas (95 % enrichment). The resulting $^{18}O^+$ SIMS depth profiles are shown in Fig. 2. It can be seen that the $^{18}O^+$ count rate reaches a maximum within about 10 nm which is caused by the carbon layer at the surface of the samples (necessary for charge compensation). A least-squares fit of the solution of the diffusion equation for a constant diffusion source (equation (1)) through the data points of the depth profiles yields the ^{18}O tracer diffusion coefficients shown in Fig. 2. The resulting oxygen diffusion length is similar in all four samples so that the evaluated ^{18}O tracer diffusion coefficients are in the range $(3-6)\times10^{-20}\,m^2s^{-1}$, and thus practically independent of the dopant element and of its concentration.

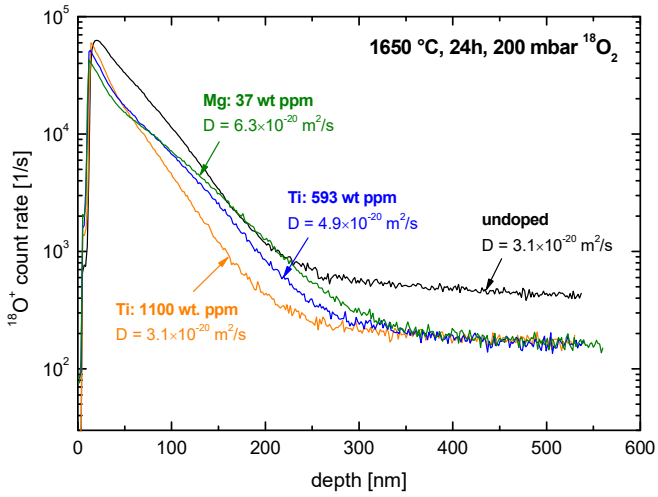

Fig. 2 Comparison of ^{18}O SIMS depth profiles of four α-Al_2O_3 samples (undoped, 593 wt ppm Ti, 1100 wt ppm Ti, 37 wt ppm Mg) which were simultaneously annealed for 24 h at 1650 °C in 200 mbar $^{18}O_2$ gas.

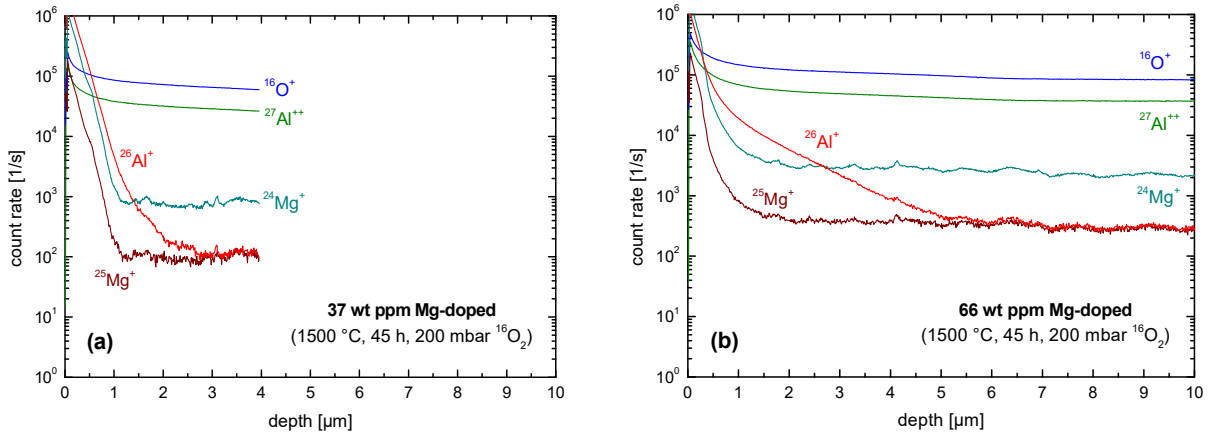

Fig. 3 SIMS raw data of ^{26}Al depth profiles in simultaneously annealed Mg-doped samples at 1500 °C, 45 h in 200 mbar $^{16}O_2$. (a) 37 wt ppm Mg-doped, (b) 66 wt ppm Mg-doped.

For the Ti-doped samples, the respective ^{26}Al diffusion data has already been published elsewhere [6]. It could be clearly demonstrated that the Al diffusivity increases with the Ti concentration up to about one order of magnitude for the highest level (about 1000 wt ppm Ti) with respect to the undoped single crystals.

^{26}Al diffusivity measurements in Mg-doped samples became very difficult because the ^{26}Al diffusivity in these samples is much lower than in the undoped samples. After 8 hours at 1500 °C the samples did not show any detectable broadening as compared to the SIMS depth profiles of the as-prepared sample. Prolonged annealing (45 hours) yielded the SIMS raw data presented in Fig. 3. The approximate evaluation of the ^{26}Al depth profile of the sample containing 37 wt ppm Mg (see Fig. 3a) yields as an upper bound for the Al diffusivity at 1500 °C a value $D_{Al} \leq 3 \cdot 10^{-19}$ m^2/s, which is two decades lower than the Al diffusivity in undoped alumina (see Fig. 5 in reference [6]). Comparing these raw data with the raw data for a Ti-doped sample (see Fig.2a in [6]) it becomes obvious that the Mg background signal is elevated due to the Mg doping and that, therefore, the dynamic range of the ^{26}Al signal is principally reduced in these samples. But a dynamic range of about four orders of magnitude (see Fig. 3) is, however, more than sufficient for tracer diffusion experiments.

Mg doping obviously slows down the bulk diffusion of ^{26}Al as compared to Ti doping. The pronounced penetration of ^{26}Al in the sample with 66 wt ppm Mg must therefore be due to a rapid diffusion path which is suggested by the exponential decay of the ^{26}Al intensity in Fig. 3b. The polysynthetic basal twins (confer Fig. 1) which were observed both by TEM and by optical microscopy are possibly representing the rapid diffusion paths. Another peculiarity of

the Mg-doped samples is the wavy background signal of Mg (see Fig. 3b) which suggests the existence of Mg-rich precipitates (e.g. $MgAl_2O_4$). Even extensive TEM work (s. section 2.2) failed, however, to supply supporting evidence for this conjecture.

Summarising, the key results of this study (this work and [6]) are:

(I) The O diffusivity in simultaneously annealed samples (24 h at 1650 °C in 200 mbar $^{18}O_2$ gas) is practically identical in undoped, in Mg-doped and in Ti-doped single crystals.

(II) Mg doping drastically reduces the Al diffusivity in α-Al_2O_3.

(III) The Al diffusivity increases with the Ti concentration. The activation energy of the Al diffusivity is about (4.0 ± 0.3) eV in the Ti-doped single crystals [6]. In our previous work (3.9 ± 0.3) eV was measured for a Ti concentration of about 300 wt ppm [17].

(IV) The activation energy of the Al diffusivity in the undoped single crystal is (3.5 ± 0.3) eV [6]. In our previous work [19] we measured (3.75 ± 0.1) eV so that there is no significant difference between the activation energy of the Al diffusion in the Ti-doped and in the undoped samples.

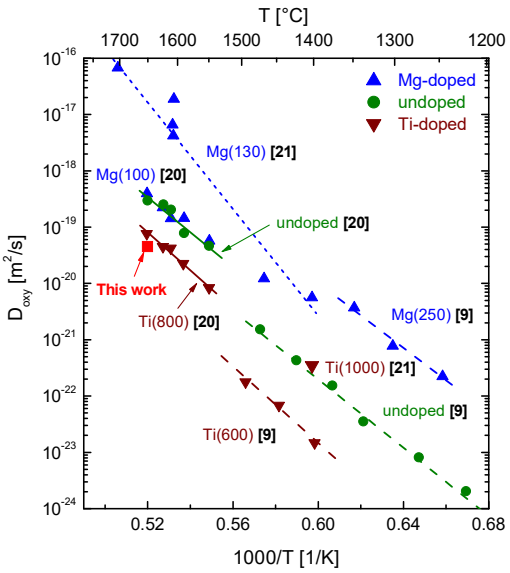

Fig. 4 Impact of Mg or Ti doping on the self-diffusion of oxygen in single crystalline α-Al_2O_3. Data from Lagerlöf et al. [9], Reddy & Cooper [20], Haneda & Monty [21]. Full green circles: nominally undoped; triangles pointing upwards: Mg-doped; triangles pointing downwards: Ti-doped; numbers in brackets: dopant concentrations in wt ppm or at. ppm (see text); red square: this work (mean value of the oxygen diffusion coefficients shown in Fig. 2).

4 Discussion

4.1 Simultaneous oxygen diffusion in differently doped samples

Surprisingly the diffusivity of oxygen was virtually identical in four differently doped samples, which were simultaneously annealed at 1650 °C in 200 mbar $^{18}O_2$ gas. The average value of the diffusion coefficients from Fig. 2 is represented as a red square in Fig. 4.

In the literature, as can be inferred from Fig. 4, the effect of Mg or Ti on the diffusivity of oxygen, D_{oxy}, in α-Al_2O_3 is not at all unambiguous [9],[20],[21]. Here we will recall only the most striking discrepancies: Reddy and Cooper [20] report that 800 wt ppm of Ti reduce D_{oxy} by half an order of magnitude as compared to nominally undoped samples while 100 wt ppm of Mg did not alter the D_{oxy} values (compared to undoped samples). Haneda and Monty [21] confirm the effect of Ti reported in [20], but find significant differences (1.5 orders of magnitude at the highest temperatures, see Fig. 4) for nearly identical Mg concentrations (100 wt ppm [20] and 130 at ppm [21], respectively). Lagerlöf et al. [9] derived values for D_{oxy} from dislocation loop shrinkage. According to their data 600 wt ppm Ti reduced D_{oxy} by one order of magnitude which is twice the effect Reddy and Cooper [20] observed for a Ti concentration of 800 wt ppm. Further, in contrast to Reddy and Cooper [20], who applied ^{18}O exchange (and a proton activation technique to measure ^{18}O depth profiles), Lagerlöf et al. [9] found a strong influence of Mg via their dislocation loop shrinkage approach as 250 wt ppm increased D_{oxy} by two orders of magnitude.

Table 3 Calculated solution energies (eV) of MgO and TiO_2 in α-Al_2O_3 per (dopant) metal ion.

MgO		
Eqn. (2), self-compensation mode	3.03 [22]	2.79 [23]
Eqn. (3), substitutional-vacancy mode	3.15 [22]	3.47 [23]
TiO_2		
Eqn. (4), substitutional-vacancy mode	3.53 [22]	3.08 [23]

The present work and the literature summary (see also Fig. 4) demonstrate that Mg and Ti doping seem to have no unambiguous effect on oxygen diffusion in single crystalline α-Al_2O_3. As MgO obviously has either no measurable effect on the oxygen diffusivity or entails some kind of increase it is appropriate to rank reaction energies obtained via computer simulations of

MgO solution reactions [22],[23] in order to identify possible transport mechanisms: While the lowest energy was found for the self-compensation mode

$$3MgO + 2Al_{Al}^{\times} \rightleftharpoons 2Mg'_{Al} + Mg_i^{\bullet\bullet} + Al_2O_3 \tag{2}$$

a similar value was found for the substitutional-vacancy mode

$$2MgO + 2Al_{Al}^{\times} + O_O^{\times} \rightleftharpoons 2Mg'_{Al} + V_O^{\bullet\bullet} + Al_2O_3 \tag{3}$$

The moderate differences of calculated solution energies per (dopant) metal ion of reactions (2) and (3) (see values compiled in Table 3, especially reference [22]) could rationalise the fact that experiments yield results which either indicate an occasional increase of the oxygen vacancy concentration (reaction (3)) or no measurable impact (reaction (2)) of Mg doping. A further complication may arise from the tendency of two substitutional magnesium ions, Mg'_{Al}, and one oxygen vacancy, $V_O^{\bullet\bullet}$, to form a neutral cluster $\left\{2Mg'_{Al} : V_O^{\bullet\bullet}\right\}^{\times}$ with calculated binding energies of 2.15 eV [5] and 2.56 eV [22].

Ti doping has very little effect on oxygen diffusion in α-Al_2O_3. The TiO_2 solution reaction (substitutional-vacancy mode, see Table 3)

$$3TiO_2 + 4Al_{Al}^{\times} \rightleftharpoons 3Ti_{Al}^{\bullet} + V_{Al}^{\prime\prime\prime} + 2Al_2O_3 \tag{4}$$

has the lowest calculated energy per dissolved foreign ion [22],[23]. Reaction (4) obviously only effects the aluminium diffusion. The intrinsic oxygen vacancy concentration is anyhow low because of the high formation energy of the Schottky equilibrium [5] (and is further diminished because of reaction (4) in combination with the Schottky formation reaction). Moreover, the high concentration of aluminium vacancies could favour clustering of aluminium and oxygen vacancies [5] and thus trap a significant fraction of the latter ones. The dependence of cluster formation on dopant concentration and on temperature could explain why in some studies Ti doping led to a decreased oxygen diffusion. For a generic example (of the analogous situation of Al diffusion in Ti-doped alumina) the reader is referred to our previous study [6].

In the light of the aforementioned arguments the published mean value of the activation energy of oxygen diffusion in obviously very different samples (6.3 eV [7]) seems to be rather an approximate parameter than a fingerprint of a well defined transport mechanism.

4.2 Al diffusion in Mg-doped samples

Mg doping entails a drastic reduction of the Al diffusivity in α-Al_2O_3 (see discussion related to Fig. 3) which turned out to be rather difficult to interpret quantitatively. As our ^{26}Al tracer diffusion experiment is the first study ever undertaken on aluminium diffusion in Mg-doped α-Al_2O_3 there are no other data available for comparison. None of the conventional approaches (see equations (2) and (3)) is suitable to explain why Mg decreases the diffusivity of aluminium.

In [6] we suggested a radically new concept and proposed the aluminium interstitial, $Al_i^{\bullet\bullet\bullet}$, as dominant species for aluminium diffusion in nominally undoped alumina. The aluminium interstitials are supposed to be injected at the liquid/solid interface because of the low oxygen potential during the crystal growth process (see reference [6] for details). Taking this concept into account one can assume that $Mg'_{Al} : Al_i^{\bullet\bullet\bullet}$ clusters [5] may trap aluminium interstitials and thus reduce the concentration of aluminium interstitials.

5 Conclusions

The present investigation was based on extremely pure α-Al_2O_3 single crystals (see Table 2) which had been deliberately doped with exactly determined amounts of TiO_2 and MgO. In order to demonstrate unambiguously the influence of the different dopants on oxygen diffusion four differently doped samples were annealed simultaneously in an $^{18}O_2$ atmosphere (200 mbar at 1650 °C). In such a crucial experiment the diffusivities in undoped and TiO_2 and MgO doped α-Al_2O_3 are identical within a factor of about 2 (see Fig. 2). This result is surprising because other groups found in some cases a fairly marked but non-uniform impact of the two dopants on oxygen diffusion. As the energies obtained in published computer simulations for the most probable dopant incorporation reactions are rather similar, it is, however, not at all surprising that in the past contradictory findings on the impact of Mg and Ti on the oxygen diffusion had been observed on samples with (different) higher impurity levels as compared to the present work.

Al self-diffusion is much more rapid than oxygen diffusion. In this study (this work and our previous investigation [6]) it is experimentally demonstrated for the first time that the Al diffusivity increases with increasing Ti concentration [6] and that Mg doping drastically reduces the Al diffusivity (this work). The impact of Ti-doping can be quantitatively rationalised taking explicitly into account cluster formation reactions together with respective published binding

energies. The surprisingly high diffusivity in undoped crystals is tentatively explained by Al interstitials, $Al_i^{\bullet\bullet\bullet}$, injected during the crystal growth process [6]. For Mg doping the interpretation of the Al diffusion data relies on cluster formation between the dopant and the Al interstitials which is supported by published calculated cluster binding energies [5].

Acknowledgements

We are indebted to Dr. Robert A. Jackson for a discussion on point defect formation energies and to Mrs. Angelika Ohlendorf for careful polishing of alumina single crystals. Financial support from Deutsche Forschungsgemeinschaft (DFG) via the grant FI 881/9-1 is gratefully acknowledged.

References

[1] J.H. Harding, K.J.W. Atkinson, R.W. Grimes, Experiment and Theory of Diffusion in Alumina, J. Am. Ceram. Soc. 86 (2003) 554–559.

[2] R.H. Doremus, Diffusion in alumina, J. Appl. Phys. 100 (2006) 101301-1–17.

[3] A.H. Heuer, Oxygen and aluminum diffusion in α-Al_2O_3: How much do we really understand?, J. Eur. Ceram. Soc. 28 (2008) 1495–1507.

[4] P. Fielitz, G. Borchardt, Self-Diffusion of the Constituent Elements in Alpha-Alumina, Mullite and Aluminosilicate Glasses, Diffusion Foundations Vol. 8, Progress in Thermodynamics, Diffusion, Ion and Proton Transport of Ionic Compounds and Ion-Conducting Polymer Films, Editor H. Mehrer, Trans Tech Publications (2016), p. 80.

[5] K.P.D Lagerlöf, R.W. Grimes, The defect chemistry of sapphire (α-Al_2O_3), Acta Mater. 46 (1998) 5689–5700.

[6] P. Fielitz, S. Ganschow, K. Kelm, G. Borchardt, Aluminium self-diffusion in high-purity α-Al_2O_3: Comparison of Ti-doped and undoped single crystals, Acta Mater. 195 (2020) 416–424.

[7] A.H. Heuer, D.B. Hovis, J.L. Smialek, B. Gleeson, Alumina Scale Formation: A New Perspective, J. Am. Ceram. Soc. 94 (2011) s146–s153.

[8] F.A. Kröger, Defect Related Properties of Doped Alumina, Solid State Ionics 12 (1984) 189–199.

[9] K.P.D. Lagerlöf, T.E. Mitchell, A.H. Heuer, Lattice Diffusion Kinetics in Undoped and Impurity-Doped Sapphire (α-Al_2O_3): A Dislocation Loop Annealing Study, J. Am. Ceram. Soc. 72 (1989) 2159–2171.

[10] V.D. Kurochkin, L.P. Kravchenko, Analysis of impurities in high-purity aluminum oxide by glow discharge mass spectrometry, Powder Metall. Met. Ceram. 45 (2006) 493–499.

[11] J.B. Bilde-Sørensen, B.F. Lawlor, T. Geipel, P. Pirouz, A.H. Heuer, K.P.D- Lagerlöf, On basal slip and basal twinning in Sapphire (α-Al_2O_3) – I. Basal Slip revisited, Acta Mater. 44 (1996) 2145–2152.

[12] T. Geipel, J.B. Bilde-Sørensen, B.F. Lawlor, P. Pirouz, K.P.D- Lagerlöf, A.H. Heuer, On basal slip and basal twinning in Sapphire (α-Al_2O_3) – III. HRTEM of the twin/matrix interface, Acta Mater. 44 (1996) 2165–2174.

[13] G.A. Keig, Influence of the valence state of added impurity ions on the observed color in doped aluminum oxide single crystals, J. Cryst Growth 2 (1968) 356–360.

[14] S.K. Mohapatra, F.A. Kröger, Defect Structure of α-Al_2O_3 Doped with Magnesium, J. Am. Ceram. Soc. 60 (1977) 141–148.

[15] P. Fielitz, G. Borchardt, M. Schmücker, H. Schneider, Al-26 diffusion measurement in 2/1-mullite by means of Secondary Ion Mass Spectrometry, Solid State Ionics 177 (2006) 493–496.

[16] J.M. Ferguson, Al^{26} Decay Scheme, Phys. Rev. 112 (1958) 1238 –1240.

[17] P. Fielitz, G. Borchardt, S. Ganschow, R. Bertram, A. Markwitz, ^{26}Al tracer diffusion in titanium doped single crystalline α-Al_2O_3, Solid State Ionics 179 (2008) 373–379.

[18] J. Crank, The Mathematics of Diffusion, 2nd ed., Oxford Univ. Press, Oxford 1975.

[19] P. Fielitz, G. Borchardt, S. Ganschow, R. Bertram, ^{26}Al tracer diffusion in nominally undoped single crystalline α-Al_2O_3, Defect and Diffusion Forum Vols. 323-325 (2012) 75–79.

[20] K.P.R. Reddy, A.R. Cooper, Oxygen Diffusion in Sapphire, J. Am. Ceram. Soc. 65 (1982) 634–638.

[21] H. Haneda, C. Monty, Oxygen self-diffusion in magnesium- or titanium-doped alumina single crystals, J. Am. Ceram. Soc. 72 (1989) 1153–1157.

[22] C.R.A. Catlow, R. James, W.C. Mackrodt, R.F. Stewart, Defect energetics in α-Al_2O_3 and rutile TiO_2, Phys. Rev. B 25 (1982) 1006–1026.

[23] R.W. Grimes, Solution of MgO, CaO, and TiO_2 in α-Al_2O_3, J. Am. Ceram. Soc. 77 (1994) 378–384.